Mössbauer Study of $ZnFe_3S_4$ and $NiFe_3S_4$ Clusters in *Pyrococcus furiosus* Ferredoxin

K. K. P. Srivastava,[†] K. K. Surerus,[†] R. C. Conover,[§] M. K. Johnson,[§] J.-B. Park,[‡] M. W. W. Adams,[‡] and E. Münck*,[†]

Department of Chemistry, Carnegie Mellon University, 4400 Fifth Avenue, Pittsburgh, Pennsylvania 15213, and Department of Biochemistry and Department of Chemistry, University of Georgia, Life Science Building, Athens, Georgia 30602

Received August 20, 1992

Pyrococcus furiosus ferredoxin is a small protein (MW 7500) containing an Fe_4S_4 cluster which readily converts into an Fe_3S_4 form. Incubation of Fe_3S_4 ferredoxin with Zn^{2+} or Ni^{2+} yields the mixed-metal clusters $[ZnFe_3S_4]^+$ and $[NiFe_3S_4]^+$. Here we report a systematic Mössbauer study of $[Fe_3S_4]^0$, $[ZnFe_3S_4]^+$, $[NiFe_3S_4]^+$, and $[NiFe_3S_4]^+$ complexed with CN^-. Two sites of $[Fe_3S_4]^0$ form a delocalized Fe^{3+}·Fe^{2+} pair whereas the third site has a localized Fe^{3+} valence state. Upon incorporation of a divalent heterometal the Fe_3S_4 fragment of the core can accommodate one additional electron, leading to a localized Fe^{2+} site in the $[ZnFe_3S_4]^+$ (cluster spin $S = {}^5/_2$) ferredoxin. We have analyzed the Mössbauer spectra taken between 1.5 and 150 K in fields up to 6.0 T in the framework of a spin Hamiltonian formalism. While the parameter sets obtained for the sites of the delocalized pair are similar to that obtained for the pair of $[Fe_3S_4]^0$, the data suggest unusual magnetic hyperfine interactions, perhaps caused by a low-lying orbital state ($\approx$200 cm^{-1}), for the Fe^{2+} site. In contrast to $[ZnFe_3S_4]^+$, the $S = {}^3/_2$ states of $[NiFe_3S_4]^+$ and its CN^- complex lack a localized Fe^{2+} site; rather, the three Fe sites display the same quadrupole splittings and isomer shifts. Analysis of the magnetic hyperfine interactions, however, reveals distinguishable sites. Isomer shift data suggest a shift of d-electron density from the Fe_3S_4 core fragment to the Ni site.

Introduction

Pyrococcus furiosus ferredoxin (*Pf* Fd)[1] is a monomeric protein, $M_r = 7500$, containing a single Fe_4S_4 cluster when isolated under anaerobic conditions.[2] The protein has three cysteine residues (cys 11, 17, and 56) in a sequence arrangement typical of those found in bacterial ferredoxins, but an aspartate residue replaces the cysteine that would normally complete the cluster coordination.[3] The iron–sulfur cluster has been shown to undergo facile and quantitative $Fe_4S_4 \leftrightarrow Fe_3S_4$ interconversion.[3] Following studies by Moura and collaborators on the formation of $CoFe_3S_4$,[4] $ZnFe_3S_4$,[5,6] $CdFe_3S_4$,[6,7] $GaFe_3S_4$[6] and $NiFe_3S_4$[6,8] clusters on *Desulfovibrio gigas* ferredoxin II (*Dg* Fd II) it has recently been shown that incubation of the 3Fe form of *Pf* Fd with excess metal ions yields quantitative generation of clusters with MFe_3S_4 cores, with M = Ni,[9] Tl,[10] Co,[11] and Zn.[11] These procedures allow site-specific incorporation of other metals into the core of the Fe_3S_4 cluster, thus generating heterometallic clusters which are interesting from a standpoint of electronic structure and bioinorganic chemistry.

Studies of the reduced, $S = 2$, state of the Fe_3S_4 cluster of *Dg* Fd II have greatly advanced our knowledge of the electronic structure of iron–sulfur clusters. In contrast to clusters with Fe_2S_2 cores which exhibit localized Fe^{3+} and Fe^{2+} sites, the mixed valence state of the $[Fe_3S_4]^0$ ($S = 2$) cluster exhibits a delocalized Fe^{3+}·Fe^{2+} pair and a localized Fe^{3+} site; the mixed-valence pair is Robin–Day class III, whereas the trapped valence Fe^{3+} is class II.[12] By analyzing the Mössbauer spectra of *Dg* Fd II, Papaefthymiou and co-workers[13] recognized that a proper description of the exchange coupling required consideration of double exchange in addition to the commonly used Heisenberg terms. These authors have also introduced a novel spin Hamiltonian for the description of double exchange.[7,13,14] Mössbauer studies of Fe_4S_4 cubanes suggest that all three accessible oxidation states of the cluster have at least one delocalized pair. Because of the large number of unknown exchange coupling parameters and the scant experimental information, a definite spin coupling scheme has not yet been established for any oxidation state of Fe_4S_4 clusters. However, a detailed model with consideration of double exchange have recently been put forward.[15,16] Moreover, Noodle-

* To whom correspondence should be addressed.
† Carnegie Mellon University.
‡ Department of Biochemistry, University of Georgia.
§ Department of Chemistry, University of Georgia.

(1) Abbreviations used: *Pf*, *Pyrococcus furiosus*; *Dg*, *Desulfovibrio gigas*; Fd, ferredoxin; ZFS, zero field splitting; EFG, electric field gradient; Smes, mesitylthiolate(1–).
(2) Aono, S.; Bryant, F. O.; Adams, M. W. W. *J. Bacteriology* **1989**, *171*, 3433–3439.
(3) Conover, R. C.; Kowal, A. T.; Fu, W.; Park, J.-B.; Aono, S.; Adams, M. W. W.; Johnson, M. K. *J. Biol. Chem.* **1990**, *265*, 8533–8541.
(4) Moura, I.; Moura, J. J. G.; Münck, E.; Papaefthymiou, V.; LeGall, J. *J. Am. Chem. Soc.* **1986**, *108*, 349–351.
(5) Surerus, K. K.; Münck, E.; Moura, I.; Moura, J. J. G.; LeGall, J. *J. Am. Chem. Soc.* **1987**, *109*, 3805–3807.
(6) Surerus, K. K. Ph.D. Thesis, University of Minnesota, 1989.
(7) Münck, E.; Papaefthymiou, V.; Surerus, K. K.; Girerd, J.-J. In *Metal Clusters in Proteins*; L. Que Jr., Ed.; American Chemical Society: Washington, DC, 1988; Vol. 372; pp 302–325.
(8) Surerus, K. K., Moura, I.; Moura, J. J. G.; Münck, E. unpublished results. Reference 6 describes the formation of a $[NiFe_3S_4]^+$ cluster in *Dg* Fd II. Originally, it was thought that the EPR spectrum of the *D. gigas* cluster was indicating the presence of an $S = {}^5/_2$ $[NiFe_3S_4]^+$ cluster in addition to the $S = {}^3/_2$ form. This conclusion was suggested by the observation of a broad, excited state $g = 4.8$ resonance (Figure 43 of ref 6) similar in shape to the signal observed for *Dg* $[ZnFe_3S_4]^+$.[5] We recognize now that the $g = 4.8$ resonance results from the excited state of the $S = {}^3/_2$ system. In fact, except for differences in line width and a minor $g = 4.3$ contaminant, the EPR spectrum of the *Dg* $[NiFe_3S_4]^+$ cluster is very similar to the spectrum shown in Figure 8A.
(9) Conover, R. C.; Park, J.-B.; Adams, M. W. W.; Johnson, M. K. *J. Am. Chem. Soc.* **1990**, *112*, 4562–4564.
(10) Fu, W.; Conover, R. C.; Park, J. B.; Adams, M. W. W.; Johnson, M. K. Manuscript in preparation.
(11) Finnegan, M.; Conover, R. C.; Park, J. B.; Adams, M. W. W.; Johnson, M. K. Manuscript in preparation.
(12) Robin, M. B.; Day, P. *Mixed Valence Chemistry—A Survey and Classification*; Academic Press: 1967; Vol. 10, pp 247–405.
(13) Papaefthymiou, V.; Girerd, J.-J.; Moura, I.; Moura, J. J. G.; Münck, E. *J. Am. Chem. Soc.* **1987**, *109*, 4703–4710.
(14) Girerd, J.-J.; Papaefthymiou, V.; Surerus, K. K.; Münck, E. *Pure Appl. Chem.* **1989**, *61*, 805–816.
(15) Noodleman, L. *Inorg. Chem.* **1991**, *30*, 246–256.
(16) Noodleman, L. *Inorg. Chem.* **1991**, *30*, 256–264.
(17) Noodleman, L.; Norman, J. G.; Osborne, J. H.; Aizman, A.; Case, D. A. *J. Am. Chen. Soc.* **1985**, *107*, 3418–3426.
(18) Noodleman, L.; Case, D. A.; Baerends, E. J. In *Theory and Applications of Density Functional Approaches to Chemistry*; Labanowski, J. K., Andzelm, J. W., Eds.; Springer-Verlag: Berlin, 1990.

0020-1669/93/1332-0927$04.00/0

man and co-workers[17,18] have studied the coupling problem of Fe_4S_4 clusters with density functional methods.

The possibility of incorporating a diamagnetic metal into the core of an Fe_3S_4 cluster offers the opportunity to explore the exchange coupling problem of cubane clusters for the simpler three-spin problem. Surerus and co-workers have shown[5,6] that incorporation of Zn^{2+}, Cd^{2+}, and Ga^{3+} into the Fe_3S_4 core allows one more electron to be added to the Fe_3S_4 fragment, thus creating a mixed-valence state with cluster spin $S = {}^5/_2$. A preliminary account of the $[ZnFe_3S_4]^+$ ($S = {}^5/_2$) cluster of *Dg* Fd II has been published.[5] Here we present a detailed Mössbauer study of the $[ZnFe_3S_4]^+$ ($S = {}^5/_2$) cluster in *Pf* Fd.

Conover and co-workers have recently reported the formation of an $[NiFe_3S_4]^+$ ($S = {}^3/_2$) cluster in *Pf* Fd;[9] this cluster binds cyanide to yield another interesting cluster state for chemical and biophysical studies. Cyanide presumably binds at the Ni site, analogous to what has been described for the cyanide-bound $[Fe_4S_4]$ cluster of *Pf* Fd.[19] The formation of a protein-bound $NiFe_3S_4$ cluster complements recent work in R. H. Holm's laboratory that has led to the syntheses of $NiFe_3S_4$ cubanes which were recently studied with a variety of spectroscopic techniques.[20,21] Here we report Mössbauer and EPR spectra of *Pf* Fd $[NiFe_3S_4]^+$ and $[NiFe_3S_4]^+$–CN. The Ni and Zn containing clusters provide an interesting contrast of electronic structure. Thus, while the Mössbauer spectra of $[ZnFe_3S_4]^+$ reflect the presence a delocalized Fe^{3+}·Fe^{2+} pair and a localized Fe^{2+} site, $[NiFe_3S_4]^+$ exhibits valence delocalization over the Fe_3S_4 fragment of the core.

Materials and Methods

Pyrococcus furiosus was grown and its ferredoxin purified as described previously.[2] ^{57}Fe-enrichment (95%) was carried out by reconstituting the 4Fe form from apoprotein[2] and conversion to the 3Fe form.[3] The Ni[9] and Zn[11] substituted forms were prepared as described. EPR spectra were recorded on an IBM ER-200D spectrometer interfaced to a Bruker 1600 computer and fitted with an Oxford Instruments ESR-9 flow cryostat. Isomer shifts are quoted relative to Fe-metal at room temperature.

Results

Spin Hamiltonian for Analyses of EPR and Mössbauer Spectra. The states to be described below have cluster spins $S = 2$, ${}^3/_2$, and ${}^5/_2$. We have analyzed the data in the framework of the spin Hamiltonian

$$H = H_e + H_{hf} \tag{1}$$

with

$$H_e = D\left\{S_z^2 - \frac{1}{3}S(S+1) + \frac{E}{D}(S_x^2 - S_x^2)\right\} + \beta \mathbf{S}\cdot\mathbf{g}\cdot\mathbf{H} \tag{2}$$

$$H_{hf} = \sum_i \{\mathbf{S}(i)\cdot\mathbf{A}(i)\cdot\mathbf{I}(i) - g_n\beta_n\mathbf{H}\cdot\mathbf{I}(i) + H_Q(i)\} \tag{3}$$

$$H_Q(i) = \frac{eQV_{zz}(i)}{12}\{3I_z^2(i) - I(I+1) + \eta(i)(I_x^2(i) - I_y^2(i))\} \tag{4}$$

In eq 2, D and E are zero field splitting (ZFS) parameters and $\mathbf{g}$ is the electronic g-tensor. For the hyperfine terms of eq 3 the sum extends over the distinguishable subsites. For some states we have found that the magnetic hyperfine tensors, $\mathbf{A}$, and the electric field gradient (EFG) tensors {principal components V_{xx}, V_{yy}, and V_{zz}; $\eta = (V_{xx} - V_{yy})/V_{zz}$}, are rotated relative to the principal axis frame of the ZFS tensors. The rotation between the frames is described by Euler angles α, β, and γ. We kept either the A- and ZFS-tensor (case 1) or the A- and EFG-tensor (case 2) in the same principal axis system.

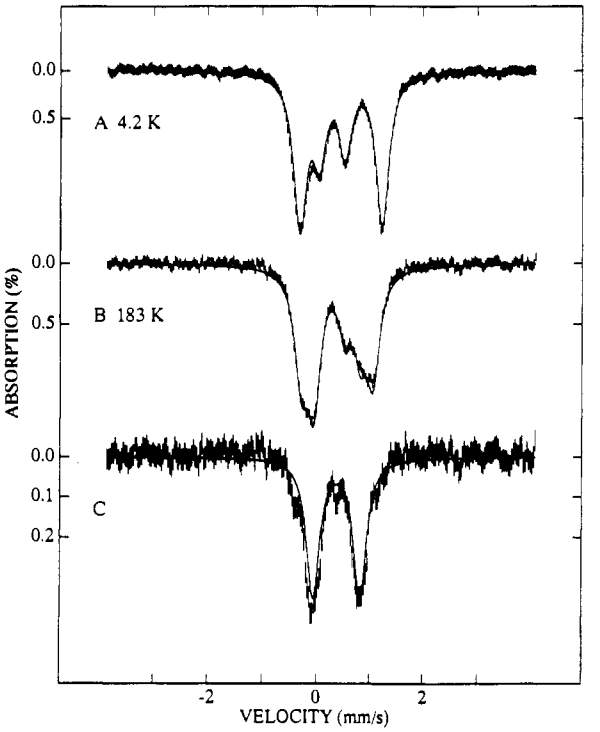

Figure 1. Zero field Mössbauer spectra of the $[Fe_3S_4]^0$ ($S = 2$) cluster of *Pf* Fd recorded at 4.2 K (A) and 183 K (B). The solid lines are the results of least squares fitting two and three doublets to spectra A and B, respectively. Spectrum C displays species X, obtained by subtraction as described in the text.

We have performed extensive computer simulations of the Mössbauer spectra. Although the programs used are capable of least squares fitting an entire data set, this option was only of limited benefit for the complex spectra discussed below. For all spectra recorded at $T \leq 4.2$ K the electronic spin was found to relax slowly on the time scale of Mössbauer spectroscopy. The methodology of analyzing spectra such as shown in Figures 2 and 4 has been described in detail.[13,22]

Mössbauer Studies of the $[Fe_3S_4]^0$ Cluster. We have studied the Fe_3S_4 cluster of *Pf* Fd in both oxidation states. Here we wish to report briefly the results obtained for the reduced ($S = 2$) state of the cluster. Figure 1 shows Mössbauer spectra recorded in the absence of an external magnetic field; low temperature spectra recorded in strong applied fields are shown in Figure 2. The spectra shown are very similar to those reported for *Dg* Fd II. Since the latter have been described in considerable detail and since a comprehensive data analysis has been reported,[13] we will briefly address here only on one salient point.

The 4.2 K spectrum of Figure 1A consists of two quadrupole doublets with a 2:1 intensity ratio. Doublet 1 + 2 (labeled I in ref 13) has $\Delta E_Q = 1.54$ mm/s and $\delta = 0.47$ mm/s; this doublet represents two identical sites which form a valence-delocalized Fe^{2+}·Fe^{3+} pair. Doublet 3 (labeled II in ref 13), with $\Delta E_Q = 0.48$ mm/s and $\delta = 0.30$ mm/s, belongs to a localized Fe^{3+} site. The temperature dependences of ΔE_Q and δ are listed in Table I. Papaefthymiou et al.[13] have reported that the spectra of the *Dg* Fd II cluster exhibit at $T > 10$ K an additional quadrupole doublet, labeled species X. The Mössbauer parameters of species X indicated that it belongs to an excited state where the excess electron of the mixed-valence state is spread equally over the three iron sites. Interestingly, species X is also observed for *Pf*

(19) Conover, R. C.; Park, J.-B.; Adams, M. W. W.; Johnson, M. K. *J. Am. Chem. Soc.* **1991**, *113*, 2799–2800.
(20) Ciurli, S.; Yu, S.-b.; Holm, R. H.; Srivastava, K. K. P.; Münck, E. *J. Am. Chem. Soc.* **1990**, *112*, 8169–8171.
(21) Zhou, J.; Scott, M. J.; Hu, Z.; Peng, G.; Münck, E.; Holm, R. H. *J. Am. Chem. Soc.* **1992**, *114*, 10843–10854.
(22) Zimmermann, R.; Münck, E.; Brill, W. J.; Shah, V. K.; Henzl, M. T.; Rawlings, J.; Orme-Johnson, W. H. *Biochim. Biophys. Acta* **1978**, *537*, 185–207.

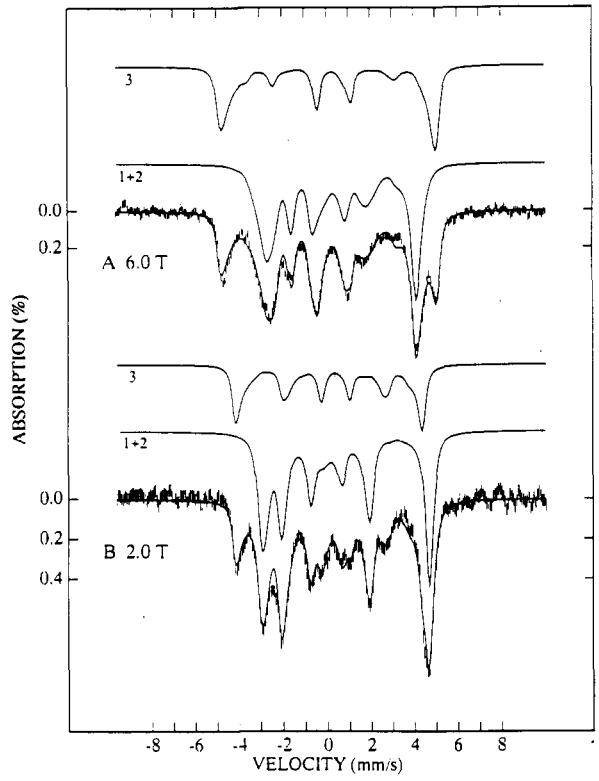

Figure 2. Spectra of the $[Fe_3S_4]^0$ ($S = 2$) cluster of *Pf* Fd recorded at 4.2 K in parallel applied magnetic fields. The solid lines are the result of spectral simulations based on eq 1 using the parameters listed in Table II. The spectral contributions of the delocalized pair, sites 1 and 2, and the Fe^{3+} site are shown separately.

Table I. Least-Squares Fitting Results of Zero-Field Spectra of the $[Fe_3S_4]^0$ Form of *Pf* Fd[a]

param	$T = 4.2$ K	$T = 50$ K	$T = 100$ K	$T = 183$ K
		Site 1 + 2		
ΔE_Q	1.54	1.50	1.44	1.34
δ	0.47	0.46	0.44	0.40
Γ	0.29	0.31	0.31	0.30
		Site 3		
ΔE_Q[b]	0.48	0.52	0.54	0.57
δ[b]	0.30	0.30	0.29	0.26
Γ	0.28	0.28	0.29	0.27
		Component X		
ΔE_Q[b]		0.92	0.90	0.88
δ[b]		0.47	0.41	0.39
Γ_L		0.25	0.26	0.29
Γ_R		0.29	0.29	0.29
%		9	16	30

[a] Units of ΔE_Q, δ, and line width Γ are mm/s, uncertainty ±0.02 mm/s. [b] Due to a lack of resolution between site 3 and component X at $T \geq 50$ K, the uncertainty in ΔE_Q and δ is ±0.1 mm/s and ±0.05 mm/s, respectively.

Fd. Its presence becomes apparent at 50 K where species X accounts for 9% of the total Mössbauer absorption. As the temperature is raised, the absorption associated with species X increases while doublets 1 + 2 and 3 seem to maintain their 2:1 intensity ratio. The solid line in Figure 1B is the result of least squares fitting the 183 K spectrum to three quadrupole doublets, with a fixed 2:1 intensity ratio for doublets 1 + 2 and 3. Figure 1C shows a representation of species X, obtained by subtracting the fitted curves for sites 1 + 2 and 3 from the data of Figure 1B.

The solid lines in Figure 2 were generated with the $S = 2$ spin Hamiltonian of eq 1, using the parameter set listed in Table II. Since we have described elsewhere in great detail the methodology of analyzing spectra such as those shown in Figure 2,[13,22] we will not comment on the analysis here. For an interpretation of the data and the introduction of a spin coupling model which incorporates double exchange for the delocalized pair the reader is referred to ref 13.

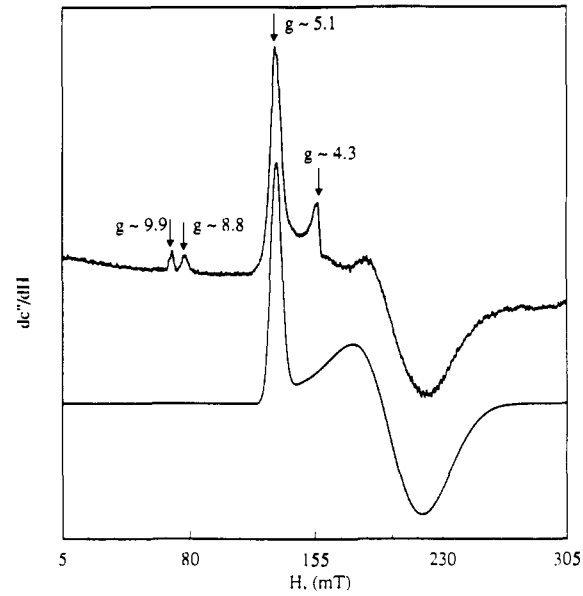

Figure 3. EPR spectrum of ^{57}Fe-enriched $[ZnFe_3S_4]^+$ of *Pf* Fd recorded at 5 K with 50 mW microwave power, 0.631 mT_{pp} modulation amplitude at 100 KHz, and 9.49 GHz frequency. This is the sample used for the Mössbauer study. Shown below the data is a simulation of the spectrum for the middle Kramers doublet using $E/D = 0.17$, $\sigma_{E/D} = 0.02$, $g_0 = (2.02, 1.975, 1.94)$ yielding $g_{eff} = (3.43, 3.01, 5.10)$.

EPR and Mössbauer Studies of $[ZnFe_3S_4]^+$. Figure 3 shows an X-band EPR spectrum of $[ZnFe_3S_4]^+$ in *Pf* Fd recorded at $T = 5$ K. The spectrum exhibits an intense absorption-type resonance at $g \approx 5.1$ and a broader derivative-type feature around $g \approx 3$. In addition the spectrum shows two weaker features at $g \sim 9.9$ and $g \sim 8.8$. As the temperature is increased the $g \sim 8.8$ resonance increases markedly in intensity. The observed resonances can be assigned to an $S = {}^5/_2$ system, described by eq 2, for which $|D| >> \beta H$ and $E/D \approx 0.17$. For E/D = 0.17 and $g = (2.02, 1.975, 1.94)$, eq 2 predicts for $D < 0$ for the three Kramers doublets the following effective g-values: $g_x = 0.21$, $g_y = 0.17$, $g_z = 9.63$ for the ground doublet, $g_x = 3.43$, $g_y = 3.01$, $g_z = 5.10$ for the middle doublet, and $g_x = 2.42$, $g_y = 8.76$, $g_z = 1.29$ for the upper doublet. (Since the cluster contains formally two ferrous ions the Zeeman term of eq 2 is not necessarily isotropic.) Variable temperature EPR shows that the $g \sim 9.9$ resonance belongs to the ground doublet; hence $D < 0$.[23] Plots of the log of the intensity ratio of the $g \sim 9.9$ and 8.8 features versus $1/T$ indicate $D = -2.1 \pm 0.3$ cm^{-1}. A simulated spectrum for the middle Kramers doublet is shown below the data of Figure 3. This simulation yields more precise g-values than could be obtained from a visual inspection of the spectra. In order to account for the width of the resonances we have assumed that the ZFS parameter E/D has a Gaussian distribution with width $\sigma_{E/D} = 0.02$. This distribution width is in agreement with the observed breadth of the excited state $g \sim 8.8$ signal.

Figures 4–7 show Mössbauer spectra of $[ZnFe_3S_4]^+$ recorded over a range of temperatures and applied magnetic fields. The spectrum of Figure 4A was recorded at 4.2 K in a parallel applied field of 50 mT. Spectra recorded in zero field and in a 50 mT transverse field were identical to that shown in Figure 4A.

(23) The spectra of all our samples contain a weak resonance around $g = 4.3$. This resonance belongs to a minority species representing probably less than 5% of the total spin concentration. A similar resonance is also observed for similarly treated *Dg* Fd II samples[5,6] although only under *reducing* conditions; it vanishes when the samples are oxidized in air or with redox dyes. This behavior suggests that the $g = 4.3$ species belongs to an $S = {}^5/_2$ cluster system, perhaps a $[ZnFe_3S_4]^+$ cluster in a somewhat different configuration.

Table II. Hyperfine Parameters of *P. furiosus* Clusters[a]

cluster	S	D, cm^{-1}	E/D	site	ΔE_Q,[b] mm/s	η	β	γ	δ,[b] mm/s	A_x, MHz	A_y, MHz	A_z, MHz	A_{av}, MHz
$[Fe_3S_4]^0$	2	−2.5(5)	0.23(2)	1 + 2	+1.54	0.4	20	0	0.47	−17(1)	−25.9(3)	−16.5(7)	−20
				3	+0.48	0.3	106	90	0.30	+16.9(7)	+17.6(9)	+14.1(3)	+16.2
$[ZnFe_3S_4]^+$	$^5/_2$	−2.1(3)	0.18(2)	1	|1.52|	0.9	33[c]	0	0.51	−14(2)	−19(3)	−14(1)	−15
				2	−1.52	0.7	115[c]	90	0.51	−9(3)	−17(1)	−17(2)	−14
				3	|3.05|[d]		∼45		0.62				<7[e]

[a] β and γ are Euler angles that rotate the EFG- and A-tensors into the ZFS-tensor frame. [b] Uncertainty ±0.02 mm/s, δ relative to Fe metal at 298 K. [c] β is distributed by ±10° for site 1 and ±5° for site 2 (see text). [d] Extrapolated from high temperature data, uncertainty ±0.1 mm/s; ΔE_Q = 2.35 mm/s at 153 K. [e] $|A_{av}| < 7$.

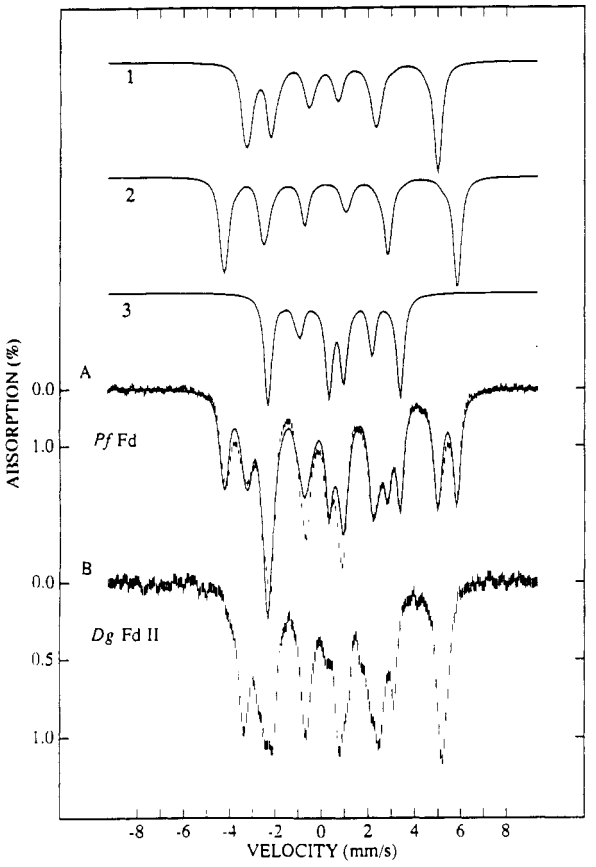

Figure 4. Mössbauer spectra of the $S = {}^5/_2$ $[ZnFe_3S_4]^+$ clusters of *Pf* Fd (A) and *Dg* Fd II (B). The spectra were recorded at 4.2 K in an applied field of 50 mT. The *Dg* Fd II spectrum is the same as that of ref 5. The solid line drawn through the data of part A is a spectral simulation based on eq 1, using for the mixed-valence pair (sites 1 and 2) the parameter set of Table II and the following hyperfine parameters for the Fe^{2+} site 3: $\Delta E_Q = -3.05$ mm/s, $\eta = -0.2$ and $H_{int} = 10.7$ T; for this particular solution the internal field is tilted by $\alpha = 75°$ and $\beta = 45°$ relative to the z-axis of the ZFS-tensor.

Identical spectra were also observed at 1.5 K. The shape of the spectra and their temperature independence between 1.5 K and 4.2 K implies that they result from an isolated Kramers doublet which is predominantly populated at 4.2 K. Since the spectra are the same in parallel and transverse field, it follows that the Kramers doublet is magnetically uniaxial; i.e. one of the principal g-values is at least 10 times larger than the other two. These conclusions are in concord with the interpretation of the EPR results.

When the temperature is increased above 4.2 K the Mössbauer spectra broaden due to increased relaxation rates of the electronic spin. At about 30 K a pattern of reasonably resolved quadrupole doublets becomes discernible. We have noticed that the spectral resolution is maximized when the samples are studied in an applied field of ca. 0.1 T. Two representative spectra are shown in Figure 5. The 50 K spectrum consists of two nested quadrupole doublets with intensity ratio of 2:1. The more intense component has ΔE_Q = 1.52 mm/s and δ = 0.51 mm/s. These parameters are quite similar to those observed for the two iron sites of the valence-

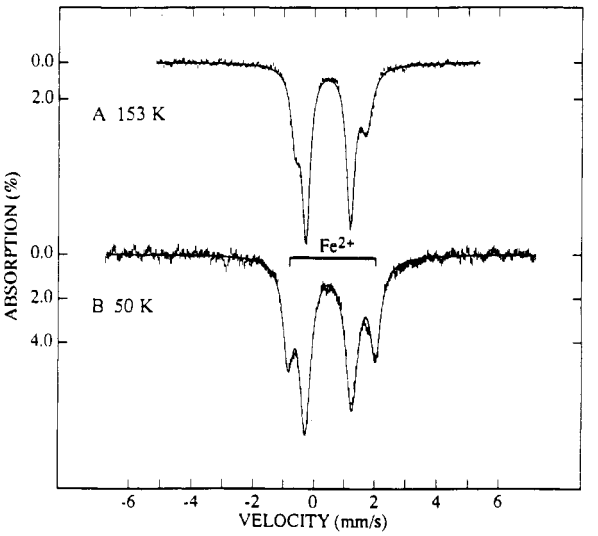

Figure 5. High-temperature Mössbauer spectra of the $S = {}^5/_2$ $[ZnFe_3S_4]^+$ cluster of *Pf* Fd. The solid lines are the result of least-squares fitting two doublets to the data.

delocalized pair of the reduced Fe_3S_4 cluster discussed above, except for a small increase of the isomer shift (see below). Within our resolution ΔE_Q of the pair is essentially independent of temperature up to 150 K. It is possible to fit the components comprising the pair with two doublets differing in ΔE_Q by 15%. This, of course, allows one to fit the spectra with narrower lines, but since the electronic system does not attain the fast relaxation limit even at 150 K, the lines are broadened by relaxation and are therefore not Lorentzian.

The second quadrupole doublet (marked by the bracket) of Figure 5B has ΔE_Q = 2.86 mm/s and δ = 0.62 mm/s at 50 K. These parameters are characteristic of high-spin ferrous ions in a tetrahedral environment of thiolate/sulfide ligands. Since this site has clearly features of a localized valence Fe^{2+} site, we will refer to it as the "Fe^{2+}" site. Thus, the cluster contains two delocalized sites at the oxidation level of (roughly) $Fe^{2.5+}$ and one Fe^{2+} site. The quadrupole splitting of the Fe^{2+} site has a pronounced temperature-dependence, showing that an excited orbital state is thermally accessible at the temperatures of the measurements; we observed ΔE_Q = 2.68 mm/s at 93 K and ΔE_Q = 2.35 mm/s at 153 K.

The 4.2 K spectrum of Figure 4A exhibits a well-resolved pattern of magnetic hyperfine interactions. As indicated by the theoretical spectra drawn above the data of Figure 4, the experimental spectrum can be decomposed into three subcomponents of equal intensity. In the following we discuss in some detail how the spectral components were identified and their parameters determined.

Because of the uniaxial nature of the ground Kramers doublet of the $S = {}^5/_2$ system, the low-field ($H < 0.1$ T) Mössbauer spectrum of each of the three subcomponents consists of six fairly narrow lines. The magnetic hyperfine interaction of each site can be described by $\mathbf{H}_{int}(i) = -\langle \mathbf{S} \rangle \cdot \mathbf{A}(i)/g_n\beta_n$, where $\langle \mathbf{S} \rangle$ is the expectation value of the electronic spin and i designates the site. For the ground Kramers doublet $\langle \mathbf{S} \rangle$ is directed along the z-axis

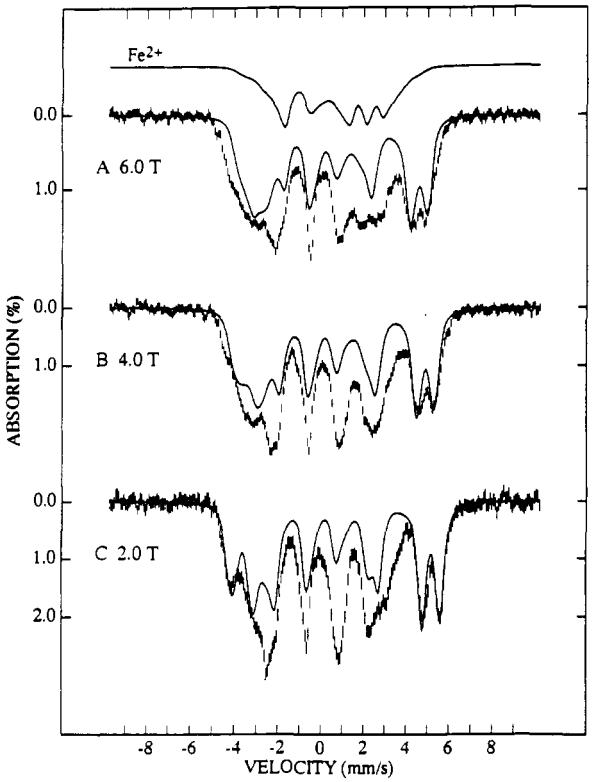

Figure 6. 4.2 K Mössbauer spectra of the $S = {}^5/_2$ $[ZnFe_3S_4]^+$ clusters of *Pf* Fd taken in strong magnetic fields applied parallel to the observed γ-radiation. The solid lines drawn through the data are theoretical curves for the mixed-valence pair (sites 1 and 2 of Table II), drawn to represent 67% of the absorption. For illustration the 6.0 T spectrum of the Fe^{2+} site is shown separately. This spectrum represents the worst match for the best "case 1" solution; at lower fields agreement with the data is better. Note that the Fe^{2+}spectrum lacks features which would be clearly discernible in the data.

of the ZFS-tensor. The magnetic hyperfine interaction for each site is specified by the internal magnetic field, H_{int} (Note that $\langle S_z \rangle = \pm g_z/4$ for weak applied fields.). The Mössbauer spectrum is then determined by specifying the principal components of the electric field gradient tensor (expressed by ΔE_Q and η), H_{int}, and angles α and β which describe the orientation of H_{int} relative to the electric field gradient tensor. It is well known that for the situation described there exists an ambiguity problem that prevents one from determining the parameters α, β, and η in a unique way.[24] Thus, a family of values for α, β,and η give rise to identical Mössbauer spectra. In strong applied magnetic fields, the electronic ground state is no longer uniaxial because of mixing of electronic states by the Zeeman term and the ambiguities can be resolved in principle. (In practice, the number of unknowns may be so large that ambiguities remain.) We have described previously in some detail a procedure to determine the parameters of multicomponent spectra for uniaxial Kramers doublets, and we have used the same procedure here.[13,22]

In order to assign the lines of the spectrum of Figure 4A to the three iron sites, it is useful to compare the spectrum of *Pf* Fd ZnFe with the corresponding spectrum of the same cluster in *Dg* Fd II[5] (see Figure 4B). The rightmost line of the latter spectrum contains the contributions of the two irons of the valence-delocalized pair. It can be seen that this line is split into two lines of equal intensity for the *Pf* cluster. The same observation applies for the leftmost line of the spectra. Thus, the two iron sites of the delocalized pair are magnetically inequivalent. It is fairly straightforward, but tedious, to decompose the spectra of the pair into components 1 and 2 shown in Figure 4A; other

(24) Van Dongen Torman, J.; Jagannathan, R.; Trooster, J. M. *Hyperfine Interact.* **1975**, *1*, 135–144.

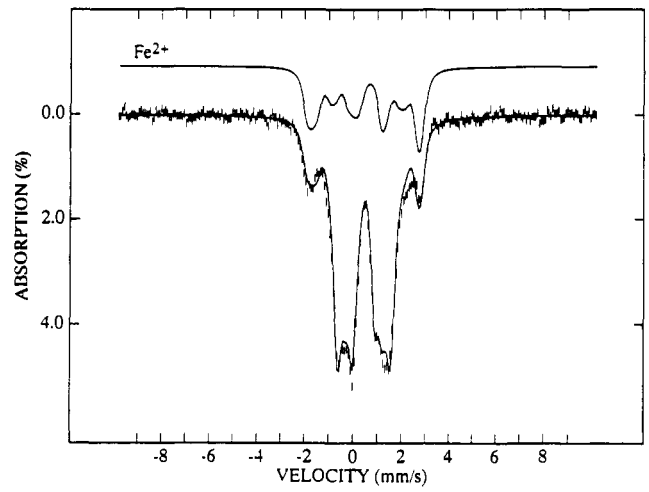

Figure 7. Mössbauer spectrum of the $S = {}^5/_2$ $[ZnFe_3S_4]^+$ cluster of *Pf* Fd recorded at 77 K in a parallel field of 6.0 T. The solid line drawn through the data is a spectral simulation using for the mixed-valence pair the parameters quoted in Table II. The spectral contribution of the Fe^{2+} site indicated separately above the data was computed with the following hyperfine parameters: $A_x = A_z = 0$, $A_y = 8$ MHz, $\Delta E_Q = +2.8$ mm/s, $\eta = 1$, and $\delta = 0.62$ mm/s, keeping the A- and EFG-tensors aligned with the ZFS tensor.

assignments of the outermost lines are in conflict with the isomer shifts and quadrupole splittings extracted from the spectra of Figure 5.

The rightmost line of the "Fe^{2+}" component is observed at a velocity of +3.5 mm/s; this line cannot be assigned to the delocalized pair. Extrapolation of the temperature dependence of ΔE_Q suggests a value of approximately 3.0 mm/s at 4.2 K. Given the position of the rightmost line it then follows that the quadrupole interaction of the ferrous site dominates the magnetic splitting at 4.2 K; i.e., H_{int} is rather small. The theoretical spectrum in Figure 4, plotted directly above the data, has $H_{int}(3) = 10.7$ T. The solid line drawn through the data is the sum of three theoretical spectra; they were simulated with the parameters listed in Table II and in the caption of Figure 4. Overall the spectra describe the data very well. A few comments, however, are appropriate here. First, the theoretical spectrum has insufficient intensity in the velocity range from −1 to +1 mm/s; the line positions, however, are correct. Probably a minor impurity contributes to the experimental spectrum in this region; it is quite impossible to change the hyperfine parameters in a way that only the intensities of the central lines are affected. Second, the leftmost lines of site 1 and 2 are broader than their rightmost lines. This broadening cannot be understood in the framework of eq 1, suggesting that at least one of the hyperfine parameters is distributed. This parameter cannot be H_{int} or ΔE_Q because a distribution of these parameters would effect all lines of the site. We have found that a distribution of angle β by $\pm 10°$ for site 1 and $\pm 5°$ for site 2 will yield the proper broadening. Third, the 4.2 K spectrum of Figure 4A results entirely from the electronic ground doublet, suggesting that $-D > 2$ cm^{-1}. Finally, the data analysis shows unambiguously that the EFG-tensors, and most probably the A-tensors as well, are rotated relative to the frame of the ZFS tensor. This is, of course, not surprising considering that the ZFS tensor refers to the cluster as a whole whereas the EFG- and A-tensors reflect the local sites. These rotations complicate the analysis of the strong field spectra considerably.

Mössbauer spectra of $[ZnFe_3S_4]^+$ recorded in strong applied magnetic fields are shown in Figure 6. Two features of the strong field data are noteworthy in the present case. First, the splitting of the magnetic components is determined by the effective field, $\mathbf{H}_{eff} = \mathbf{H}_{int} + \mathbf{H}$. Thus, by observing whether the magnetic splitting increases or decreases with increasing applied field the sign of the components of the A-tensor can be determined. Second, a strong

applied field will mix the electronic levels of the $S = {}^5/_2$ system. This mixing depends on the magnitude of the ZFS and thus leads to the determination of the parameter D. As the field is increased, $\langle S_x \rangle$ increases and the internal field tilts away from the electronic z-direction.

At 77 K the electronic spin system approaches the fast relaxation limit. For fast relaxation the internal magnetic field is given by $\mathbf{H}_{int} = -\langle \mathbf{S} \rangle_{th} \cdot \mathbf{A}/g_n\beta_n$, where $\langle \mathbf{S} \rangle_{th}$ is the thermal average of S. For $D = -2.1$ cm^{-1}, $E/D = 0.18$, and $H = 6.0$ T the thermal averages along x, y, and z are -0.30, -0.28, and -0.33, respectively. Knowledge of these expectation values allows one to estimate A-tensor components from the 77 K spectrum.

The spectrum shown in Figure 7 was recorded at 77 K in a parallel applied field of 6.0 T. The central feature of the spectrum is mainly due to the Fe sites of the delocalized pair. Its observed splitting corresponds to an effective field of about 2.5 T. Hence, the components of the A-tensor of the pair are all negative and have a magnitude of ca. 16 MHz. For clarity, a theoretical spectrum of the Fe^{2+} site is shown above the data of Figure 7. In order to match the splittings of the experimental spectrum of the Fe^{2+} site, at least one component of the A-tensor has to be positive. Since the A-tensor components of high-spin ferrous sites generally have the same sign (we are not aware of any exceptions) one could proceed with the assumption that this observation holds for the Fe^{2+} site as well.[25] However, as discussed below the present situation may be more complex.

Since $\langle \mathbf{S} \rangle_{th}$ is nearly isotropic at 77 K one can analyze the shape of the spectrum of the Fe^{2+} site by ignoring rotations of the A- and EFG-tensors relative to the ZFS-tensor. The spectrum of Figure 7 indicates that the ferrous A-tensor has $A_x \approx 0$, $A_y \approx +8$ MHz, and $|A_z| < 7$ MHz (where x, y, and z refer to the frame of the EFG-tensor). A theoretical spectrum for $\Delta E_Q = +2.8$ mm/s, $\eta = 1$, $A_x = A_z = 0$ and $A_y = +8$ MHz is shown above the data of Figure 7; the spectrum of the pair was simulated with the parameters listed in Table II.

We have made considerable efforts to fit the high-field spectra of Figure 6. We have found a reasonably consistent parameter set for the two iron sites of the delocalized pair. A satisfying description of the Fe^{2+} component, however, has been a challenge that we have not yet overcome. We know from experience that fitting of high-field Mössbauer spectra of a single high-spin ferrous site with low symmetry is a formidable task. In low symmetry the number of unknowns is substantial. For symmetries lower than rhombic there are three A-tensor components, two EFG-tensor components, and six Euler angles to be determined; in addition the A-tensor may have anti-symmetric components.[26,27] We have, therefore, made the simplifying assumption that only one set of Euler angles is required to describe the orientation of the A- and EFG-tensor relative to the ZFS-tensor. For case 1 we assumed that the A-tensor of the high-spin Fe^{2+} site is collinear with the ZFS tensor and that the EFG-tensor is rotated. Since A- and EFG-tensor components of Fe^{2+} sites are quite correlated, this model is somewhat unrealistic. For case 1 we found a parameter set that fits the entire data set fairly well. However, this solution gave an A-tensor that had positive as well as negative components ($A_x = -4$ MHz, $A_y = +12$ MHz, $A_z = -6$ MHz). Although one cannot strictly rule out such A-values (mixing of multiplets by ZFS terms could produce A-tensors quite distinct from those observed for monomeric sites; see below), we are not quite satisfied with this particular solution. We believe that the quoted A-tensor components would reflect an Fe^{2+} site for which the spin Hamiltonian approximation may be inadequate. For case 2 we have assumed that the A- and EFG-tensor of the Fe^{2+} site are collinear but rotated together relative to the ZFS tensor; this situation will apply if the symmetry of the Fe^{2+} site is not lower than rhombic. After reviewing many attempts to simulate the high-field spectra of the Fe^{2+} site, we have concluded that none of the parameters sets is sufficiently reliable to be included in Table II. On the other hand, the parameters for the mixed-valence pair represents the entire data set reasonably well; even the features of the 77 K high-field spectrum of Figure 7 are reproduced with good accuracy. The theoretical curves in Figure 6, showing the contributions of the pair, were obtained with the parameters quoted in Table II. Although we did not obtain reliable values for the A-tensor components of the Fe^{2+} site, we can put some constraints on $A_{av} = (A_x + A_y + A_z)/3$, namely $|A_{av}| < 7$ MHz; at least one A-tensor component is positive while another component seems to be ≈ 0. For comparison, ferrous rubredoxin has $A_x = -27.4$ MHz, $A_y = -11.4$ MHz, and $A_z = -51.6$ MHz.[28] Analysis of the spectrum of Figure 4 shows that the z-axis of the EFG-tensor of the Fe^{2+} is tilted by $\beta = 40$–$50°$ relative to the z-axis of the ZFS-tensor, no matter whether case 1 or case 2 was assumed. For illustration, we have shown in Figure 6 the 6.0 T spectrum for the case 1 "solution". Parallel with this study we have analyzed the spectra of the $[ZnFe_3S_4]^+$ cluster of *Dg* Fd II and the same problems were encountered.

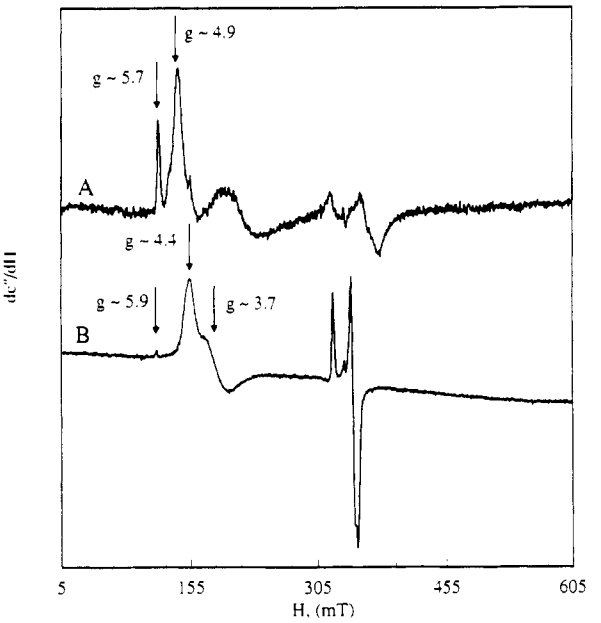

Figure 8. EPR spectra of (A) $[NiFe_3S_4]^+$ recorded at 9 K and (B) $[NiFe_3S_4]^+$–CN recorded at 34 K. Instrumental conditions: 50 mW microwave power, 0.631 mT_{pp} modulation amplitude at 100 KHz, and 9.44 GHz frequency.

Mössbauer Studies of $[NiFe_3S_4]^+$ and $[NiFe_3S_4]^+$–CN. As shown previously, upon incubation of $[Fe_3S_4]^0$ with Ni^{2+}, the heterometal is incorporated into the open site of the Fe_3S_4 cluster.[9] Conover et al.[9] have reported that the resulting $[NiFe_3S_4]^+$ cluster in *Pf* Fd has an $S = {}^3/_2$ ground multiplet with ZFS parameters $D = -2.2 \pm 0.2$ cm^{-1}, $E/D = 0.18$, and $g = 2.0$. An EPR spectrum of the sample used for the Mössbauer study is shown in Figure 8A.

Low temperature Mössbauer spectra of $[NiFe_3S_4]^+$ are shown in Figure 9. The observation of magnetic hyperfine interactions

(25) Positive A-tensor components are expected from a simple consideration of the spin coupling problem. It is interesting that the ground-state spins of all MFe_3S_4 clusters studied thus far can be predicted by using the following rule.[21] Take the dimer spin of the delocalized Fe^{2+}-Fe^{3+} pair as $S_{12} = {}^9/_2$, as shown for the Fe_3S_4 cluster of *Dg* Fd II.[13] Parallel coupling of S_3 (here the spin of the Fe^{2+} site) with the spin of M (here $S_4 = 0$) yields S_{34}. Finally, antiparallel coupling of S_{12} and S_{34} yields the system spin S. For the present case these considerations imply that S_3 is oriented antiparallel to the system spin $S = {}^5/_2$, and thus the A-tensor components of Fe^{2+} should be positive.

(26) Oosterhuis, W. T.; Lang, G. *Phys. Rev.* **1969**, *178*, 439–456.

(27) *Electron Paramagnetic Resonance of Transition Ions*; Abragam, A., Bleaney, B., Ed.; Clarendon Press: Oxford, England, 1970; pp 742–760.

(28) Winkler, H.; Kostikas, A.; Petroulease, V.; Simopoulos, A.; Trautwein, A. X. *Hyperfine Interact.* **1986**, *29*, 1347–1350.

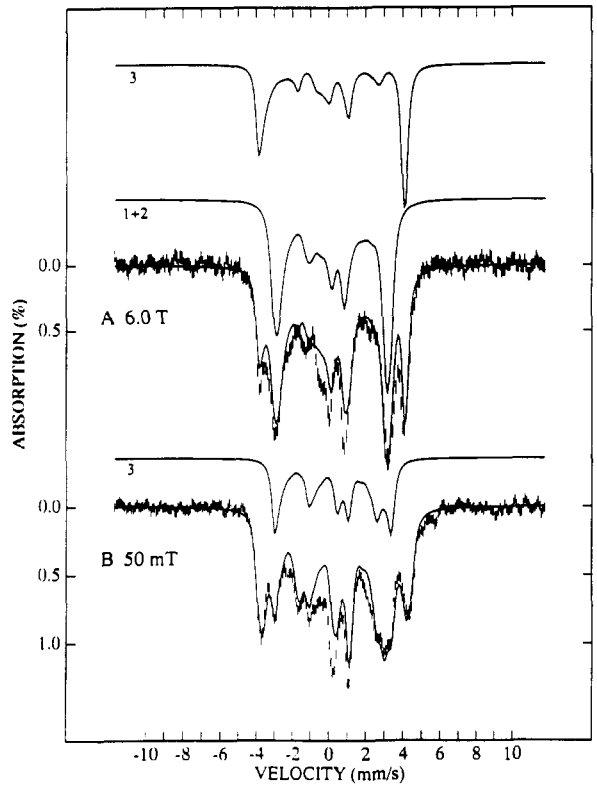

Figure 9. 4.2 K Mössbauer spectra of the $S = {}^3/_2$ $[NiFe_3S_4]^+$ cluster of *Pf* Fd. The solid lines are theoretical spectra generated from eq 1 with the parameters listed in Table III. The 6.0 T spectra for sites 1 + 2 and site 3 and the 50 mT spectrum for site 3 are shown separately above the data.

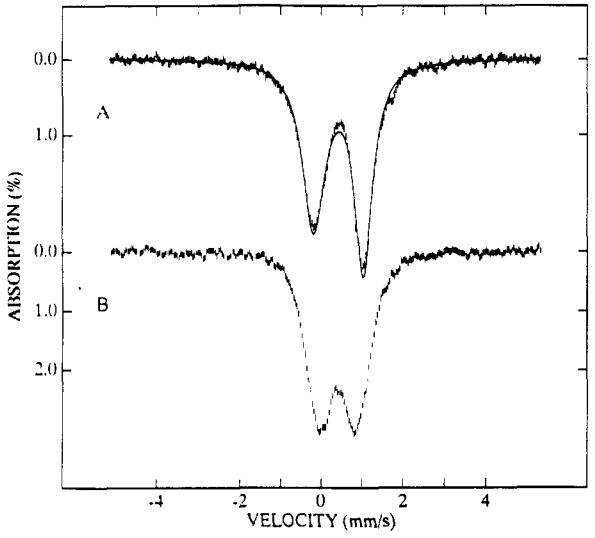

Figure 10. Zero field Mössbauer spectra of $[NiFe_3S_4]^+$ (A) and its cyanide complex (B), recorded at 170 K. The solid line in part A is a least-squares fit to a quadrupole doublet with $\Delta E_Q = 1.22$ mm/s and $\delta = 0.45$ mm/s and $\Gamma_l = 0.67$ mm/s, $\Gamma_r = 0.54$ mm/s linewidth.

in the spectrum of Figure 9A proves that the electronic spin is relaxing slowly on the time scale of Mössbauer spectroscopy. Above ca. 10 K the absorption lines broaden due to an increased electronic relaxation rate. At $T \geq 150$ K the electronic relaxation is nearly in the fast fluctuation regime and a quadrupole doublet is observed. A spectrum of $[NiFe_3S_4]^+$ *Pf* Fd recorded at 170 K is shown in Figure 10A. It consists of one quadrupole doublet with $\Delta E_Q = 1.22$ mm/s and $\delta = 0.45$ mm/s; the asymmetry and the fairly broad lines reflect, at least in part, remnant relaxation effects. In contrast to $[ZnFe_3S_4]^+$ the high-temperature spectra of $[NiFe_3S_4]^+$ lack the trapped-valence "Fe^{2+}" site, and it thus appears that the three Fe sites are equivalent as judged by ΔE_Q and δ. The low temperature spectra, however, reveal that the iron sites are magnetically distinct. Thus, the 4.2 K spectra reveal two sites with negative A-values, reminiscent of the delocalized pair of $[Fe_3S_4]^0$, and one site with an A-tensor having positive components.

Inspection of the EPR spectrum of the material used for the Mössbauer study reveals the presence of some clusters (ca. 10%) in the $[Fe_4S_4]^+$ state. Although there was no evidence from EPR of such a cluster in the "Fe_3S_4" form that was used to prepare $NiFe_3S_4$, some Fd molecules may have formed a Fe_4S_4 cluster by cannibalization of iron from other clusters during the incubation procedure with Ni^{2+}. We have recorded Mössbauer spectra at 4.2 K and 1.5 K in parallel applied fields of 0.05, 2.0, 4.0, and 6.0 T. For the 0.05 and 6.0 T spectra we have recorded reference spectra of the *Pf* Fd $[Fe_4S_4]^+$ and we have subtracted its contribution, to represent 10% of the absorption, from the spectra shown in Figure 9.

We have analyzed the spectra with the spin Hamiltonian of eq 1 for $S = {}^3/_2$ using the parameter $E/D = 0.18$ obtained from EPR but keeping D as a variable. We obtained adequate fits to the spectra by keeping all tensors collinear. The solid lines in Figure 9 are theoretical spectra generated with the parameter set of Table III. Shown above the 6.0 T spectrum of Figure 9A are theoretical spectra of the sites; since the spectra of sites 1 and 2 are nearly identical, we have plotted their sum. For identification we have shown also the 0.05 T spectrum of site 3; site 3 has $A > 0$ and its absorption lines move outward with increasing applied field. Overall the theoretical curves match the entire data set quite well.

Conover et al.[9] have shown that addition of KCN to *Pf* Fd $[NiFe_3S_4]^+$ yields a new $S = {}^3/_2$ complex with $E/D = 0.06$ and $D > 0$. Plots of the log of the intensity ratio of the $g \sim 5.9$ and 4.4 features versus $1/T$ indicate $D = +3.0 \pm 1.0$ cm^{-1}. An EPR spectrum of the sample used for our Mössbauer studies is shown in Figure 8B. The EPR features in the $g = 2$ region revealed signals at $g = 2.09$, 1.95, and 1.92. These g-values are characteristic of the $S = {}^1/_2$ state of CN^--complexed Fe_4S_4 clusters.[9] Quantitation of this $S = {}^1/_2$ signal suggests that ca. 10% of the clusters of the sample are in this state. We have completed an extensive Mössbauer study of the $[Fe_4S_4]^+$–CN form, and we have subtracted the appropriate spectra, corresponding to 10% of the total Mössbauer absorption, from our data; the resulting spectra are shown in Figure 11. The contribution of the $[Fe_4S_4]^+$–CN cluster is entirely hidden under the main absorption of the $S = {}^3/_2$ cluster; we have indicated its contribution in Figure 11C.

The spectra of Figure 11 contain another minority species (perhaps 10% of the total ^{57}Fe in the sample). Its contribution is clearly discernible in the low field Mössbauer spectra (arrows in Figure 11). Its splitting does not match any cluster in *Pf* Fd that we have studied. However, its behavior in applied magnetic fields suggests an EPR-active half-integer spin species. Yet, the EPR spectrum of Figure 8B does not indicate such a species. It is, however, conceivable that it belongs to a second $S = {}^3/_2$ form with similar EPR behavior as the majority species.

The theoretical curves in Figure 11 are the result of spectral simulations using the parameter set listed in Table III. Given that the raw data contained contributions from at least two minority species, the simulations represent the data quite well. Again, the spectra reflect two sites with $A < 0$ (sites 1 and 2) and site 3 with $A > 0$. Adequate simulations were obtained by assuming that sites 1 and 2 have identical spectra.

A few comments may be appropriate here. First, the A-tensor components of all cluster forms studied here were determined relative to the anisotropic electronic system. Thus, the components are spatially correlated, e.g. the x-component of the A-tensors of iron subsites 1, 2, and 3 refer to the same spatial direction.

Table III. Hyperfine Parameters of *P. furiosus* $[NiFe_3S_4]^+$ Clusters[a]

cluster	D, cm^{-1}	E/D	site	ΔE_Q,[b] mm/s	η	δ,[b] mm/s	A_x, MHz	A_y, MHz	A_z, MHz	A_{av}, MHz
Pf Fd	−2.2(2)	0.18(2)	1	−1.4[c]	−4.7	0.50	−18(4)	−25(4)	−22.5(3)	−22
			2	−1.4[c]	−5.7	0.50	−18(4)	−25(5)	−24.1(7)	−22
			3	−1.4[c]	−3.4	0.50	+15(1)	+19(3)	+18.1(3)	+19
Pf Fd-CN	+4(1)[d]	0.06(2)	1 + 2	−1.1[c]	−1.5	0.50	−18.5(7)	−24.7(7)	−25(7)	−23
	+3(1)[e]		3	−1.1[c]	−1.5	0.50	+13.7(7)	+19.2(7)	+19(7)	+17
$(PPh_3)(Smes)_3$	+4(1)	0.11	1	−0.6		0.48	−8(3)	−23(3)	−(4–18)	
			2	−1.1		0.48	−20(4)	−23(4)	−(14–33)	
			3	−0.82		0.48	+19(1)	+19(1)	+4(3)	+14
$(PPh_3)(SEt)_3$	>0	0.12	1	−0.90		0.47	−10.7	−17.8	−18.5	−16
			2	−0.90		0.47	−19.5	−21.7	−23.3	−22
			3	0.90		0.47	+13.4	+18.8	+19.9	+17

[a] For comparison the parameters for $[NiFe_3S_4(PPh_3)(Smes)_3]^{2-}$ [21] and $[NiFe_3S_4(PPh_3)(SEt)_3]^{2-}$ [20] are listed. All four derivatives have $S = {}^3/_2$. [b] Uncertainty ±0.02 mm/s, δ relative to Fe metal at 298 K. [c] Extrapolated from high temperature data, uncertainty ±0.2 mm/s. [d] Determined by Mössbauer spectroscopy. [e] Determined by EPR spectroscopy.

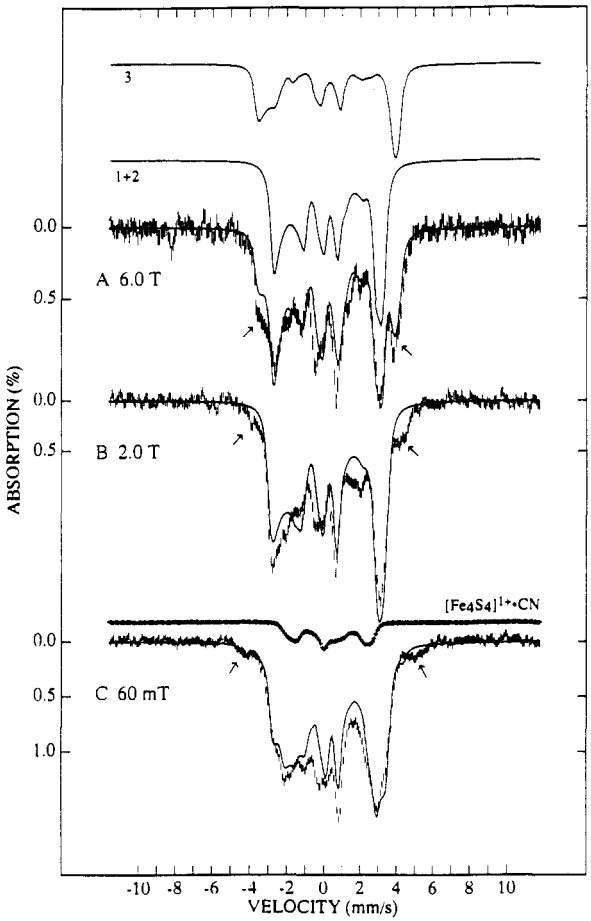

Figure 11. 4.2 K Mössbauer spectra of the $S = {}^3/_2$ $[NiFe_3S_4]^+$–CN complex of *Pf* Fd. The solid lines are theoretical spectra generated for eq 1 with the parameters listed in Table III. We have subtracted from the raw data a 10% contribution of the $S = {}^1/_2$ form of $[Fe_4S_4]^+$–CN ferredoxin, indicated in part C. The sample contains also an as yet unidentified species (ca. 10%); its outer features are indicated by the arrows. Also shown are the theoretical spectra of sites 1 + 2 and site 3 for the 6.0 T spectrum.

However, there are no spatial correlations between the corresponding components of different cluster forms; in the absence of single crystal EPR data the orientations of the ZFS tensors remain unknown. Given the complexity of decomposing the powder spectra of three subsites, the sign (ΔE_Q) and the asymmetry parameter η are essentially undetermined. Except for very favorable circumstances changes of η can be compensated by adjustments of the A-values. In Table III we have quoted estimated uncertainties for the A-tensor components: these uncertainties contain errors introduced by uncertainties in the EFG-tensor components.

Discussion

The Mössbauer spectra of the reduced Fe_3S_4 cluster of the *Pf* Fd are essentially identical to those reported for that of *Dg* Fd II. Analysis of the spectra of *Dg* Fd II has revealed that the cluster contains a valence-delocalized Fe^{2+}·Fe^{3+} pair and a trapped valence Fe^{3+} site.[13] Analysis of the spin coupling showed that double-exchange interactions lead to a parallel alignment of the electronic spins of the two iron sites to yield a dimer spin $S_{12} = {}^9/_2$. Soon after Moura et al.[4] incorporated Co^{2+} into the vacant site of the cluster to afford $[CoFe_3S_4]^{+,2+}$, Surerus and co-workers generated $[ZnFe_3S_4]^+$, $[CdFe_3S_4]^+$, $[GaFe_3S_4]^{2+}$, and $[NiFe_3S_4]^+$ clusters in *Dg* Fd II.[5-7] Incorporation of the diamagnetic Zn^{2+} reduces the negative charge of the cluster by one unit if one assumes that an anionic ligand (presumably Asp-14 or OH^- for *Pf* Fd and Cys-11 for *Dg* Fd II) binds to the Zn^{2+}. Reduction of negative charge increases the redox potential allowing one more electron to be added to the Fe_3S_4 fragment of the core. The Mössbauer spectra show clearly that this electron is added to the Fe^{3+} site which then becomes the localized-valence Fe^{2+} site, labeled here "Fe^{2+}". Surerus et al.[29] have reported recently new integer-spin EPR and Mössbauer data for the oxidized P-clusters of nitrogenase. In discussing the possibility that the P-clusters are a supercluster consisting of two bridged cubanes, these authors, drawing on the present work on $[ZnFe_3S_4]^+$, have pointed out that the charge of the supercluster would be reduced relative to the charge of two separate $Fe_4S_4(cys)_4$ clusters if cysteines would be used as bridging ligands. Such bridging could then explain the apparent low oxidation state of the cluster state P^N. We have just learned that the P-clusters may indeed consist of such bridged cubanes.[30]

The mixed-valence pair of *Pf* Fd $[Fe_3S_4]^0$ ($S = 2$) consists of two irons indistinguishable by Mössbauer spectroscopy; even the highly resolved spectra of Figure 2 do not indicate any differences between the sites. While the similarity between the sites is nearly preserved for *Dg* $[ZnFe_3S_4]^+$ [5] the two sites are readily distinguishable in the *Pf* $[ZnFe_3S_4]^+$ cluster. However, a comparison of the magnetic hyperfine tensors of the pair for $[Fe_3S_4]^0$ and $[ZnFe_3S_4]^+$ cluster forms (see Table II) shows that the electronic structures of the pair are quite similar. This suggests that $S_{12} = {}^9/_2$ for both cluster forms (with perhaps some $S_{12} = {}^7/_2$ admixture).

A comparison between the isomer shifts of the two cluster forms is instructive. Relative to $[Fe_3S_4]^0$ the isomer shift of each of the irons of the delocalized pair of $[ZnFe_3S_4]^+$ has increased by 0.04 mm/s. The shift of the Fe^{2+} site, on the other hand, is about 0.08 mm/s less than those reported for the FeS_4 sites of reduced rubredoxin and desulforedoxin. This indicates some

(29) Surerus, K. K.; Hendrich, M. P.; Christie, P. D.; Rottgardt, D.; Orme-Johnson, W. H.; Münck, E. *J. Am. Chem. Soc.* **1992**, *114*, 8579.
(30) Kim, J.; Rees, D. C. *Science* **1992**, *257*, 1677–1682.
(31) Kissinger, C.; Adman, E.; Sieker, L.; Jensen, L. *J. Am. Chem. Soc.* **1988**, *110*, 8721–8725.

d-electron transfer from the Fe^{2+} site to the pair. It also suggests that the coupling between the Fe^{2+} site and the Fe sites of the pair has some double exchange character (see also Noodleman[15,16]).

As pointed out above, we have not yet found a reliable set of hyperfine parameters for the Fe^{2+} site of $[ZnFe_3S_4]^+$. If the symmetry of the site would be lower than rhombic all tensors would have different principal axis systems, and finding a parameter set compatible with all recorded spectra may be unmanageably complex. Even if the symmetry is not lower than rhombic, the spin Hamiltonian of eq 1 may break down under certain circumstances. In the following we will discuss some of the possibilities.

In the absence of an X-ray structure of *Pf* Fd $[ZnFe_3S_4]^+$, the geometry of the Fe^{2+} site remains unknown. There are, however, good reasons to believe that the site is geometrically not unusual. The X-ray structure of $[Fe_3S_4]^+$ *Dg* Fd II shows that all three iron sites have cysteine coordination with normal bond length and angles.[31] The spectroscopic data of the various MFe_3S_4 forms of *Pf* Fd and *Dg* Fd II indicate that the heterometal (or a fourth Fe) occupies the empty site with no major structural rearrangements at the other iron sites. The spectroscopic properties of the Fe^{2+} sites of the $[ZnFe_3S_4]^+$ clusters of the two proteins are essentially the same. We have shown above that the quadrupole splitting of the Fe^{2+} site is temperature-dependent. With the reasonable assumption that the two lowest orbital states are e levels, the observed temperature dependence of ΔE_Q implies a splitting Δe of slightly less than 200 cm^{-1}; this is more than a factor of 2 smaller than the splittings reported for other iron–sulfur proteins.[32-34] The smaller splitting, reflecting perhaps a site symmetry *higher* than those usually observed, could have profound spectroscopic consequences. For instance, a rhombic distortion with the two-fold axes rotated by 45° relative to the cubic axes[35] can produce a situation where the first excited orbital e state contributes to the zero-field splitting of the ground manifold of the Fe^{2+} site. If the excited e state is as low in energy as observed here, the mixing of the e levels by spin-orbit interactions could be so pronounced that the spin Hamiltonian approximation breaks down. Even if the spin Hamiltonian approximation for the Fe^{2+} site were still reasonably good, a large zero-field splitting of the Fe^{2+} site may mix configurations of total cluster spin S, with the result that the ground manifold is a mixed-spin state (S is not a good quantum number). Sage and co-workers have analyzed such mixing ("D/J mixing") for the simpler case of the exchange-coupled binuclear iron cluster of purple acid phosphatase.[36] The good description of the EPR data by eq 2 seems to suggest that the spin Hamiltonian of eq 1 is a good approximation for the description of $[ZnFe_3S_4]^+$. However, it has been demonstrated[36] for the binuclear iron clusters that the *g*-values are considerably less sensitive to "D/J mixing" than the A-tensors. Moreover, by analyzing the effects of "D/J mixing" on the hyperfine interactions of $[Fe_3S_4]^+$ ($S = {}^1/_2$) clusters we have noticed that this mixing affects different iron sites in drastically different ways, producing even "A-tensors" with positive and negative components for high-spin ferric sites.[37] We do not have proof that such mixing is at the root of our present problems with the Fe^{2+} site, but the possibility needs to be considered.[38]

Bertrand and co-workers[34,39] have analyzed the Mössbauer and EPR data of reduced rubredoxin, desulforedoxin and reduced Fe_2S_2 clusters with respect to the properties of the Fe^{2+} sites. They have suggested that the orbital ground state of the Fe^{2+} sites have essentially d_{z^2} symmetry, with some $d_{x^2-y^2}$ admixtures. A pure d_{z^2} orbital has $\Delta E_Q \approx -3$ mm/s and $\eta = 0$. Our best "solutions" for the Fe^{2+} site have indeed a negative ΔE_Q and a small value of η. However, we cannot exclude solutions with other η values nor can we exclude positive value for ΔE_Q.

It is quite obvious that a spin coupling model for $[ZnFe_3S_4]^+$ will have to proceed along the same lines as that proposed for the $S = 2$ state of the *Dg* Fd II Fe_3S_4 cluster, with the exception that some weak double exchange between the Fe^{2+} site and the two Fe sites of the delocalized pair may need to be incorporated (see also Noodleman[15,16]). For the development of a spin coupling model knowledge of the magnetic hyperfine interactions of the Fe^{2+} site is essential. It is unlikely that further attempts to fit the Mössbauer spectra will yield an unambiguous set of hyperfine parameters for the Fe^{2+} site. ENDOR has been attempted for the *Dg* Fd II $[ZnFe_3S_4]^+$ cluster, but the EPR signal could not be saturated even at 2 K. ENDOR studies of the *Pf* Fd ZnFe cluster are in preparation. Incorporation of Cd^{2+} and Ga^{3+} into the core of the Fe_3S_4 cluster of *Dg* Fd II produced $S = {}^5/_2$ cluster forms which exhibit Mössbauer and EPR spectra nearly identical to those of *Dg* $[ZnFe_3S_4]^+$.[6] These cluster states may be useful targets of ENDOR studies as well. Finally, Holm and co-workers have synthesized a series of complexes with MFe_3S_4 cores (M = Co,[21] Ni,[21] V,[40-43] Mo,[44,45] W,[44,45] Re[46,47]). A suitable model complex for $[ZnFe_3S_4]^+$ could provide some crucial structural and spectroscopic information.

Recent studies have shown that the $[Fe_3S_4]^0$ core has a substantially higher affinity for Zn^{2+} than for Fe^{2+}.[48] This raises the question of whether proteins with $ZnFe_3S_4$ cores exist in nature, and what strategies one might want to employ to investigate their presence. The most useful signature is probably the $g = 4.3$ resonance of the $S = {}^5/_2$ form of the cluster. This raises immediately the question whether the signal would not be overwhelmed by the ever present $g = 4.3$ signals of rhombic high-spin Fe^{3+}. However, while the $g = 4.3$ signals of monomeric Fe^{3+} sites are observed for the *oxidized* state of the metal site, the signal of $[ZnFe_3S_4]^+$ originates from the *reduced* form of the cluster. Thus, one could use EPR to examine samples of whole cells, cell extracts and protein fractions under suitable reducing conditions (e.g. hydrogen gas, dithionite). While it is true that fractions of some Fe^{3+}-based EPR signals persist even at potentials as low as −500 mV (vs NHE) one could get further evidence for the presence of a $ZnFe_3S_4$ cluster by oxidizing samples whereupon the $g = 4.3$ signal of $[ZnFe_3S_4]^+$ will vanish while those of Fe^{3+} will persist or increase in intensity. Although the $[ZnFe_3S_4]^{2+}$ cluster can be obtained by mild oxidation under anaerobic conditions[6,11] (yielding a state with integer spin), oxidation with

(32) Dunham, W. R.; Bearden, A. J.; Salmeen, I. T.; Palmer, G.; Sands, R. H.; Orme-Johnson, W. H.; Beinert, H. *Biochim. Biophys. Acta* **1971**, *253*, 134–152.
(33) Münck, E.; Debrunner, P. G.; Tsibris, J. C. M.; Gunsalus, I. C. *Biochemistry* 1972, *11*, 855–863.
(34) Bertrand, P.; Gayda, J.-P. *Biochim. Biophys. Acta* **1988**, *954*, 347–350.
(35) Varret, F. *J. Phys.* **1976**, *37*, C6-437–C6-456.
(36) Sage, J. T.; Xia, Y.-M.; Debrunner, P. G.; Keough, D. T.; de Jersey, J.; Zerner, B. *J. Am. Chem. Soc.* **1989**, *111*, 7239–7247.
(37) Papaefthmiou, V.; Münck, E. Unpublished results.
(38) Consideration of mixing of spin multiplets by ZFS terms may be important for the analysis of the magnetic hyperfine interactions of Fe_4S_4 clusters. For the mixed valence state of Fe_2S_2 clusters the effects of "D/J mixing" can be detected by observation of anisotropic magnetic hyperfine interactions of the Fe^{3+} site.[50] $[Fe_4S_4]^+$ clusters, on the other hand, have two Fe^{2+} sites and a mixed valence Fe^{2+}-Fe^{3+} pair and thus have intrinsically anisotropic A-tensors. Thus, moderate "D/J mixing" will be difficult to separate from intrinsic anisotropies. Systematic magnetic susceptibility studies designed to detect excited state multiplets are clearly desirable.
(39) Bertrand, P.; Gayda, J.-P. *Biochim. Biophys. Acta* **1979**, *579*, 107–121.
(40) Kovacs, J. A.; Holm, R. H. *J. Am. Chem. Soc.* **1986**, *108*, 340–341.
(41) Kovacs, J. A.; Holm, R. H. *Inorg. Chem.* **1987**, *26*, 702–711.
(42) Kovacs, J. A.; Holm, R. H. *Inorg. Chem.* **1987**, *26*, 711–718.
(43) Carney, M. J.; Kovacs, J. A.; Zhang, Y.-P.; Papaefthmiou, G. C.; Spartalian, K.; Frankel, R. B.; Holm, R. H. *Inorg. Chem.* **1987**, *26*, 719–724.
(44) Zhang, Y.-P.; Bashkin, J. K.; Holm, R. H. *Inorg. Chem.* **1987**, *26*, 694–702.
(45) Holm, R. H.; Simhon, E. D. In *Molybdenum Enzymes*; Spiro, T. G., Ed.; Wiley-Interscience: New York, 1985; Chapter 1.
(46) Ciurli, S.; Carney, M. J.; Holm, R. H.; Papaefthymiou, G. C. *Inorg. Chem.* **1989**, *28*, 2696.
(47) Ciurli, S.; Carrie, M.; Holm, R. H. *Inorg. Chem.* **1990**, *29*, 3493.
(48) Butt, J. N.; Armstrong, F. A.; Breton, J.; George, S. J.; Thomson, A. J.; Hatchikian, E. C. *J. Am. Chem. Soc.* **1991**, *113*, 6663–6670.

air or ferricyanide will remove the Zn from the cluster's core to yield the $[Fe_3S_4]^+$ cluster state. This then yields the characteristic $g = 2.01$ signal below 20 K. It should also be noted that observation of the $g = 4.3$ resonance of the $[ZnFe_3S_4]^+$ clusters of the ferredoxins from *D. gigas* and *P. furiosus* requires temperatures below 50 K whereas most Fe^{3+} signals can still be observed at substantially higher temperatures. These procedures could be supplemented with other spectroscopic techniques once some reasonable degree of purification has been achieved. Of course, even if a protein with a $ZnFe_3S_4$ cluster can be isolated, the question of biological relevance would still need to be addressed.

The two Ni-containing clusters studied here have the same core oxidation levels as $[ZnFe_3S_4]^+$. Most conspicuous is the absence of a localized Fe^{2+} site. This observation is in accord with those reported recently for two synthetic complexes with $[NiFe_3S_4]^+$ cores.[20,21] The high temperature Mössbauer spectra of the Ni-containing clusters exhibit *one* quadrupole doublet. Although the spectral resolution is somewhat limited because none of the complexes reaches the fast fluctuation limit of the electronic spin at the highest temperature examined, the evidence is accumulating that the three iron sites of $[NiFe_3S_4]^+$ clusters are equivalent when only quadrupole splittings and isomer shifts are considered. In contrast, examination of the magnetic hyperfine interactions reveals that the Fe-sites are inequivalent. Sites 1 and 2 have A-tensors similar to those of the mixed-valence pair of $[Fe_3S_4]^0$ and $[ZnFe_3S_4]^+$. Although site 3 lacks the quadrupolar and isomer shift properties of a localized Fe^{2+} site, it has positive A-tensor components showing that the spin of site 3 is oriented antiparallel to the $S = {}^3/_2$ system spin. Whether the characterization of sites 1 and 2 as a delocalized pair with substantial double exchange is still appropriate needs to be examined with a suitable spin coupling model; see for instance ref 49.

The parameters listed in Table III reveals close similarities between the parameters of the protein-bound and the synthetic clusters. Inspection of Table III may suggest that the three iron sites of the $[NiFe_3S_4(PPh_3)(Smes)_3]^{2-}$ synthetic complex have distinguishable ΔE_Q values. As pointed out above, it is exceedingly difficult in certain circumstances to determine the EFG-tensor components by analysis of the magnetically split spectra. The low temperature data analysis[21] of the spectra of the $[NiFe_3S_4(PPh_3)(Smes)_3]^{2-}$ synthetic complex was carried out without biasing the procedure with the assumption that the ΔE_Q values are the same for all sites (In view of these difficulties the authors of ref 21 have chosen not to quote the asymmetry parameter η.). There seems to be one genuine difference between the parameters of the protein-bound clusters and the $[NiFe_3S_4(PPh_3)(Smes)_3]^{2-}$ synthetic complex; namely, A_z of site 3 of the synthetic complex is distinctly smaller than any of the site 3 components of the *Pf* Fd cluster.

The average isomer shift of the three iron sites of $[ZnFe_3S_4]^+$ is $\delta_{av} = 0.55$ mm/s. This compares well with those for $[Fe_4S_4]^+$ if we average the shifts of the mixed-valence pair and one of the Fe^{2+} sites. The protein-bound and synthetic $[NiFe_3S_4]^+$ clusters, on the other hand, have distinctly smaller shifts suggesting that electron density has been transferred from the iron sites to the Ni, suggesting a bias towards Ni^+ and participation of the Ni site in the redox chemistry of the cluster.[21]

Acknowledgment. This work was supported by the NSF (DMB9096231 to E.M., DMB9105150 to M.W.W.A., and DMB8921986 to M.K.J. and by a Research Group Training Award, DIR-9014281, to the Center for Metalloenzyme Studies at the University of Georgia) and the NIH (GM45597 to M.W.W.A. and GM33806 to M.K.J.).

(49) Blondin, G.; Borshch, S.; Girerd, J.-J. *Comments Inorg. Chem.* **1992**, *12*, 315–340.
(50) Fox, B. G.; Hendrich, M. P.; Surerus, K. K.; Andersson, K. K.; Froland, W. A.; Lipscomb, J. D.; Münck, E. *J. Am. Chem. Soc.* in press.